crystals

MDPI

Article

Properties of Sm-Doped $SrCl_2$ Crystalline Scintillators

Daisuke Nakauchi [1,*], Yutaka Fujimoto [2], Takumi Kato [1], Noriaki Kawaguchi [1] and Takayuki Yanagida [1]

[1] Division of Materials Science, Nara Institute of Science and Technology (NAIST), 8916-5 Takayama, Ikoma 630-0192, Nara, Japan; kato.takumi.ki5@ms.naist.jp (T.K.); n-kawaguchi@ms.naist.jp (N.K.); t-yanagida@ms.naist.jp (T.Y.)

[2] Department of Applied Chemistry, Graduate School of Engineering, Tohoku University, 6-6 Aramaki, Aoba, Sendai 980-8579, Miyagi, Japan; yutaka.fujimoto.c3@tohoku.ac.jp

* Correspondence: nakauchi@ms.naist.jp

Abstract: Sm-doped $SrCl_2$ crystals were prepared, and the scintillation properties such as emission spectra, decay profiles, and pulse height were investigated. Under X-ray irradiation, a broad band can be observed at 680 nm, which indicates that the major origin is due to 5d-4f transitions of Sm^{2+}. The decay curve is approximated by one exponential function with a decay time of 10 μs, and the decay time constant is typical for Sm^{2+}. From the pulse height of ^{137}Cs γ-rays, 0.1% Sm:$SrCl_2$ shows a light yield of 33,000 photons/MeV.

Keywords: scintillation; photoluminescence; near-infrared luminescence

check for updates

Citation: Nakauchi, D.; Fujimoto, Y.; Kato, T.; Kawaguchi, N.; Yanagida, T. Properties of Sm-Doped $SrCl_2$ Crystalline Scintillators. *Crystals* **2022**, *12*, 517. https://doi.org/10.3390/cryst12040517

Academic Editors: Riccardo Cerulli and Hong Joo Kim

Received: 28 February 2022
Accepted: 6 April 2022
Published: 8 April 2022

Publisher's Note: MDPI stays neutral with regard to jurisdictional claims in published maps and institutional affiliations.

1. Introduction

A scintillator is a material that exhibits luminescence when excited by ionizing radiation and is used with a photodetector to convert emitted photons into electrical signals. Scintillators play an important role in radiation measurements such as medicine [1,2], resource exploration [3], security [4], astrophysics [5], and monitoring [6,7]. Conventionally, scintillators that exhibit ultraviolet or visible luminescence, suitable for general Si-based photodiodes or photomultiplier tubes, have mainly been developed [8–10]. On the other hand, scintillators with near-infrared (NIR) luminescence have been attracting attention. Wavelengths from 650 to 950 nm, called the first optical window, are transparent to water and blood in the human body [11,12]. Hence, in vivo dosimetry during radiotherapy [13,14] and monitoring of drug delivery [15,16] have been suggested as promising applications. In addition, high-dose monitoring applications have been proposed. When monitoring high-dose environments such as nuclear reactors, radiation damage to semiconductor components hinders stable measurement. Therefore, remote monitoring using optical fiber has been proposed, and NIR photons have an advantage due to their high transmittance for optical fiber [17,18]. In addition, it is easy to distinguish red-NIR photons from Cherenkov light generated in a nuclear reactor because Cherenkov light, characterized by pale light, is known to have high light intensity in the near-ultraviolet to visible regions [19,20]. On the other hand, in high-dose field measurements using conventional ultraviolet–visible scintillators, Cherenkov light inhibits stable measurements.

Alkaline earth halides doped with divalent rare-earth ions, as represented by Eu:SrI_2 [21–25], exhibit high-scintillation LY and high energy resolution, and Sm^{2+} has been recently attracting attention as an emission center showing red-NIR photons [26–28]. So far, there have been few reports of radioluminescence (RL) from Sm^{2+}-doped materials [29–34]. The properties of Sm-doped $SrCl_2$ have not yet been clarified, despite its relatively low deliquescence, ease of growth, and adequate bandgap energy (~5.2 eV [35]). In this study, we focused on Sm-doped $SrCl_2$ crystals as a red-NIR scintillator and investigated the scintillation properties.

2. Materials and Methods

Sm-doped $SrCl_2$ single crystals were synthesized using a vertical Bridgman furnace (VFK-1800, Crystal Systems, Yamanashi, Japan). The initial concentrations of tested Sm were 0.1, 0.5, and 1%. $SrCl_2 \cdot 6H_2O$ (99%), $SmCl_3$ (99.9%), and carbon powders were vacuumed (~10 Pa) in a quartz ampoule and then sealed using a gas burner (KSA-22, Tokyo Koshin Rikagaku Seisakusho, Tokyo, Japan). Here, the carbon powder maintains the reduction conditions to remove residual oxygen contamination and promote the reduction of $Sm^{3+} \rightarrow Sm^{2+}$ [36]. Then, crystal growth was performed using the Bridgman furnace with a pulling speed of 10 mm/h. The samples were processed into smaller samples, and the actual concentrations were determined using X-ray fluorescence (XRF) analyses (SEA-1000A, SII, Chiba, Japan). The tested tube voltage and used filters were 50 kV with a Pb filter, 30 kV with a Pb filter, and 15 kV with a Cr filter.

Photoluminescence (PL) properties were evaluated using spectrofluorometers (C11347 and C11367, Hamamatsu Photonics, Shizuoka, Japan). Radioluminescence (RL) spectra under X-ray irradiation, RL decay profiles, and pulse height were measured according to a previously reported setup [37,38]. The photomultiplier tube with a multialkali photoelectric surface used at pulse height covered the sensitivity of 300–900 nm, and the quantum efficiency (QE) was 18% at 520 nm and 10% at 680 nm.

3. Results and Discussion

The sizes of 0.1, 0.5, and 1% Sm:$SrCl_2$ synthesized by the Bridgman method were approximately 4–6 mmφ × 10–15 mm, and they had a few cracks owing to the high pull-down speed. For following characterizations, the samples were cut into small pieces with a size of 2–3 mmφ × 1 mm, and the surfaces were polished. The actual Sm concentrations of the 0.1, 0.5, and 1% Sm:$SrCl_2$ samples are 0.043, 0.186, and 0.315%, respectively. In all samples, the selected pieces showed lower Sm concentrations than the initial concentrations because of segregation. Figure 1 shows the appearance of the prepared Sm:$SrCl_2$. The appearance of the sample is transparent, and red luminescence is observed when irradiated with an ultraviolet lamp (365 nm). X-ray fluorescence spectra of 0.1% Sm:$SrCl_2$ sample with a tube voltage of (top) 50 kV, (middle) 30 kV, and (bottom) 15 kV are shown in Figure S1.

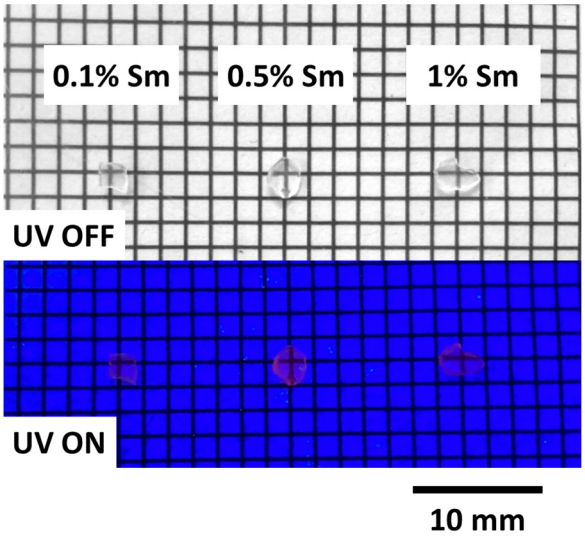

Figure 1. Photographs of Sm:$SrCl_2$.

Figure 2 shows the PL 3D spectrum of the 0.1% Sm-doped sample, and the 0.1, 0.5, and 1% doped samples show QYs of 85.9%, 65.7%, and 39.4%, respectively. Under excitation from 290 to 680 nm, a broad emission band is observed at 680 nm The spectral features are almost the same as those in Sm:$SrBr_2$ [28]. Figure 3 shows the PL decay profiles monitored at 680 nm when excited at 280 nm. The obtained curves are fitted with an exponential

function, which indicates the emission has the decay time constants of 9–11 μs. The origin is the 5d-4f transitions of Sm^{2+} because the decay time constants are close to those reported in previous studies [28]. The decrease in QY indicates concentration quenching, while the decay does not change. The results suggest that the radiative transition rate decreases, and the nonradiative transition rate increases as the Sm-concentration increases.

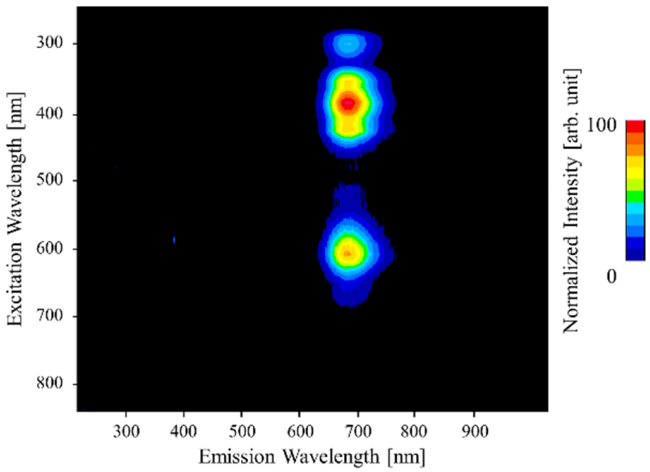

Figure 2. PL 3D spectrum of 0.1% Sm:$SrCl_2$.

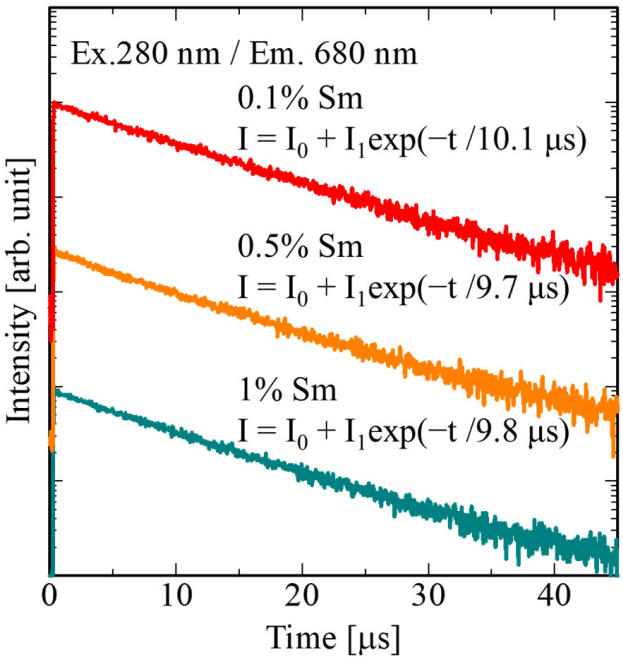

Figure 3. PL decay curves of Sm:$SrCl_2$.

Figure 4 shows the RL spectra of Sm:$SrCl_2$ crystals. The samples dominantly exhibit an emission band at 680 nm due to Sm^{2+}. In addition, a broad emission band is observed at 430 nm, which is due to self-trapped excitons [39]. The emission decreases with the concentration of doped Sm. According to PL analyses, the wavelength of STE luminescence overlaps with the absorption wavelength of Sm^{2+}, and the absorption decreases STE luminescence. In addition, all samples exhibit a few sharp peaks in the range from 550 to 610 nm, and the origin is the 4f-4f transitions of Sm^{3+}. Figure 5 shows the RL decay curves of the Sm:$SrCl_2$ crystals. The obtained curves are approximated with one exponential function, which indicates that the decay times are about 9 μs. The values are shorter than PL decay, and this trend was also observed in other materials. One reason is thought to be the interaction of numerous excited secondary electrons leading to quenching.

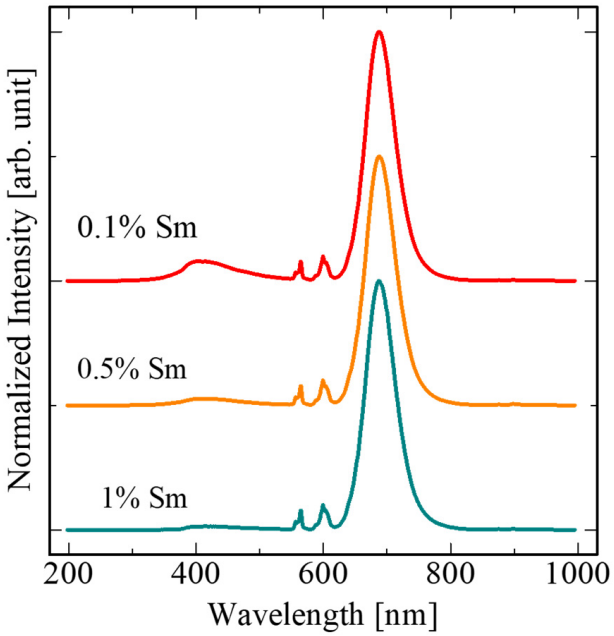

Figure 4. RL spectra of Sm:$SrCl_2$.

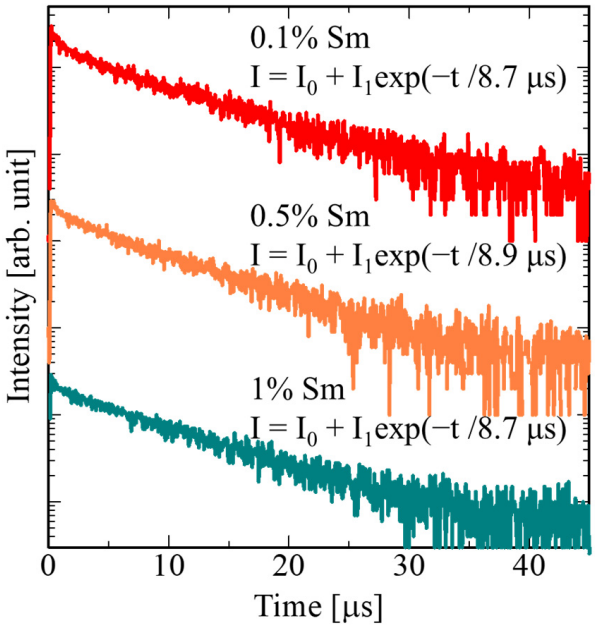

Figure 5. RL decay curves of Sm:$SrCl_2$.

Figure 6 shows the pulse height spectra of Sm:$SrCl_2$ under ^{137}Cs (662 keV γ-rays) exposure. Ce:$Y_3Al_5O_{12}$ was selected as a reference sample showing an RL peak at 520 nm with an LY of 20,000 photons/MeV [40]. The light yields (LYs) of the samples were calculated as follows: LY = 20,000 × ($channel_{sample}$/$channel_{ref}$) × (18%/10%), calculated considering the photoabsorption peak channel and spectral sensitivity of the used photomultiplier tube. The LYs are 33,000 for 0.1%, 28,000 for 0.5%, and 24,000 photons/MeV for 1% Sm:$SrCl_2$ crystals. Among the samples, the 0.1% doped sample shows the highest LY. This value is higher than Sm:$Ba_{0.3}Sr_{0.7}Cl_2$ (22,000), Sm:$SrBr_2$ (32,000) and Eu:$SrBr_2$ (25,000), while it is lower than Sm, Eu:SrI_2 (~40,000), Eu:SrI_2 (80,000) and Yb:SrX_2 (~50,000) [22,23,31,34,41]. The LYs increase with increasing QYs, and the LYs are dependent on the QYs. The trend of the results are consistent with the Robbins and Lempicki models [42,43].

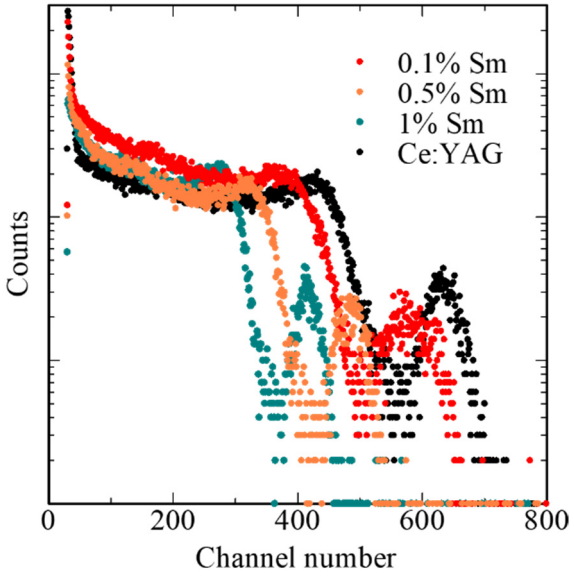

Figure 6. Pulse height spectra of ^{137}Cs γ-rays.

4. Conclusions

Sm-doped $SrCl_2$ crystals were prepared to investigate the properties for scintillator applications. Sm:$SrCl_2$ shows a broad peak at 680 nm due to Sm^{2+}. The decay curves are approximated with an exponential function, and the decay time constant is typical of Sm^{2+}. The PL QY and LY of the 0.1% $SmSrCl_2$ sample are higher than the other presented samples. Sm:$SrCl_2$ exhibits a comparable LY (33,000 photons/MeV) in comparison with conventional scintillators such as Tl:NaI and Ce:Lu_2SiO_5, and the LYs are high enough to measure γ-rays.

Supplementary Materials: The following supporting information can be downloaded at: https://www.mdpi.com/article/10.3390/cryst12040517/s1, Figure S1: X-ray fluorescence spectra of 0.1% Sm:$SrCl_2$ sample with a tube voltage of (top) 50 kV, (middle) 30 kV, and (bottom) 15 kV.

Author Contributions: Conceptualization, D.N. and T.Y.; methodology, D.N. and Y.F.; investigation, D.N.; resources, D.N.; data curation, D.N.; writing—original draft preparation, D.N.; writing—review and editing, T.K. and N.K.; supervision, N.K. and T.Y.; project administration, D.N.; funding acquisition, N.K. and T.Y. All authors have read and agreed to the published version of the manuscript.

Funding: This work was supported by Grant-in-Aid for Scientific Research B (19H03533, 21H03733, and 21H03736) and Early-Career Scientists (20K20104) from the Japanese Society of Applied Physics (JSPS). Foundation from Japan Science and Technology Agency (JST) A-STEP (JPMJTM20FP), Cooperative Research Project of Research Center for Biomedical Engineering, Nippon Sheet Glass Foundation, SEI Group CSR Foundation, TEPCO Memorial Foundation, KRF Foundation, and Murata Science Foundation are also acknowledged.

Institutional Review Board Statement: Not applicable.

Informed Consent Statement: Not applicable.

Data Availability Statement: Not applicable.

Conflicts of Interest: The authors declare no conflict of interest.

References

1. Yamamoto, S.; Okumura, S.; Kato, N.; Yeom, J.Y. Timing measurements of lutetium based scintillators combined with silicon photomultipliers for TOF-PET system. *J. Instrum.* **2015**, *10*, T09002. [CrossRef]
2. Ishikawa, A.; Yamazaki, A.; Watanabe, K.; Yoshihashi, S.; Uritani, A.; Sakurai, Y.; Tanaka, H.; Ogawara, R.; Suda, M.; Hamano, T. Development of optical-fiber-based neutron detector using Li glass scintillator for an intense neutron field. *Sens. Mater.* **2020**, *32*, 1489–1495. [CrossRef]

3. Melcher, C.L. Scintillators for well logging applications. *Nucl. Instrum. Methods Phys. Res. B* **1989**, *40*, 1214–1218. [CrossRef]
4. Glodo, J.; Wang, Y.; Shawgo, R.; Brecher, C.; Hawrami, R.H.; Tower, J.; Shah, K.S. New Developments in Scintillators for Security Applications. *Phys. Procedia* **2017**, *90*, 285–290. [CrossRef]
5. Itoh, T.; Yanagida, T.; Kokubun, M.; Sato, M.; Miyawaki, R.; Makishima, K.; Takashima, T.; Tanaka, T.; Nakazawa, K.; Takahashi, T.; et al. A 1-dimensional γ-ray position sensor based on GSO:Ce scintillators coupled to a Si strip detector. *Nucl. Instrum. Methods Phys. Res. A* **2007**, *579*, 239–242. [CrossRef]
6. Salonen, L. A rapid method for monitoring of uranium and radium in drinking water. *Sci. Total Environ.* **1993**, *130*, 23–35. [CrossRef]
7. Shirakawa, Y. Development of a direction finding gamma-ray detector. *Nucl. Instrum. Methods Phys. Res. B* **2007**, *263*, 58–62. [CrossRef]
8. Dorenbos, P. The quest for high resolution γ-ray scintillators. *Opt. Mater. X* **2019**, *1*, 100021. [CrossRef]
9. Kim, C.; Lee, W.; Melis, A.; Elmughrabi, A.; Lee, K.; Park, C.; Yeom, J.-Y. A Review of Inorganic Scintillation Crystals for Extreme Environments. *Crystals* **2021**, *11*, 669. [CrossRef]
10. Kumar, V.; Luo, Z. A Review on X-ray Excited Emission Decay Dynamics in Inorganic Scintillator Materials. *Photonics* **2021**, *8*, 71. [CrossRef]
11. Weissleder, R. A clearer vision for in vivo imaging. *Nat. Biotechnol.* **2001**, *19*, 316–317. [CrossRef] [PubMed]
12. Quek, C.-H.; Leong, K.W. Near-Infrared Fluorescent Nanoprobes for in Vivo Optical Imaging. *Nanomaterials* **2012**, *2*, 92–112. [CrossRef] [PubMed]
13. Mijnheer, B.; Beddar, S.; Izewska, J.; Reft, C. In vivo dosimetry in external beam radiotherapy. *Med. Phys.* **2013**, *40*, 070903. [CrossRef] [PubMed]
14. Frangioni, J. In vivo near-infrared fluorescence imaging. *Curr. Opin. Chem. Biol.* **2003**, *7*, 626–634. [CrossRef] [PubMed]
15. Sapre, A.A.; Novitskaya, E.; Vakharia, V.; Cota, A.; Wrasidlo, W.; Hanrahan, S.M.; Derenzo, S.; Makale, M.T.; Graeve, O.A. Optimized scintillator YAG:Pr nanoparticles for X-ray inducible photodynamic therapy. *Mater. Lett.* **2018**, *228*, 49–52. [CrossRef]
16. Wang, H.; Lv, B.; Tang, Z.; Zhang, M.; Ge, W.; Liu, Y.; He, X.; Zhao, K.; Zheng, X.; He, M.; et al. Scintillator-Based Nanohybrids with Sacrificial Electron Prodrug for Enhanced X-ray-Induced Photodynamic Therapy. *Nano Lett.* **2018**, *18*, 5768–5774. [CrossRef]
17. Kobayashi, M.; Kondo, K.; Hirabayashi, H.; Kurokawa, S.; Taino, M.; Yamamoto, A.; Sugimoto, S.; Yoshida, H.; Wada, T.; Nakagawa, Y.; et al. Radiation damage of BGO crystals due to low energy γ rays, high energy protons and fast neutrons. *Nucl. Instrum. Methods Phys. Res.* **1983**, *206*, 107–117. [CrossRef]
18. Gurzhiev, A.N.; Turchanovich, L.K.; Vasil'chenko, V.G.; Bogatyrjov, V.A.; Mashinsky, V.M. Radiation damage in optical fibers. *Nucl. Instrum. Methods Phys. Res. A* **1997**, *391*, 417–422. [CrossRef]
19. Dai, X.; Rollin, E.; Bellerive, A.; Hargrove, C.; Sinclair, D.; Mifflin, C.; Zhang, F. Wavelength shifters for water Cherenkov detectors. *Nucl. Instrum. Methods Phys. Res. A* **2008**, *589*, 290–295. [CrossRef]
20. Cao, X.; Jiang, S.; Jia, M.; Gunn, J.; Miao, T.; Davis, S.C.; Bruza, P.; Pogue, B.W. Observation of short wavelength infrared (SWIR) Cherenkov emission. *Opt. Lett.* **2018**, *43*, 3854–3857. [CrossRef]
21. Kimura, H.; Kato, T.; Nakauchi, D.; Kawaguchi, N.; Yanagida, T. Radiation-induced Luminescence Properties of SrBr2 Transparent Ceramics Doped with Different Eu Concentrations. *Sens. Mater.* **2020**, *32*, 1381–1387. [CrossRef]
22. Sekine, D.; Fujimoto, Y.; Koshimizu, M.; Nakauchi, D.; Yanagida, T.; Asai, K. Photoluminescence and scintillation properties of Yb^{2+}-doped $SrCl_2$ crystals. *Jpn. J. Appl. Phys.* **2020**, *59*, 012005. [CrossRef]
23. Mizoi, K.; Arai, M.; Fujimoto, Y.; Nakauchi, D.; Koshimizu, M.; Yanagida, T.; Asai, K. Photoluminescence and scintillation properties of Yb^{2+}-doped $SrCl_{2-x}Br_x$ (x = 0, 1.6, 2.0) crystals. *Appl. Phys. Express* **2020**, *13*, 112008. [CrossRef]
24. Cherepy, N.J.; Hull, G.; Drobshoff, A.D.; Payne, S.A.; Van Loef, E.; Wilson, C.M.; Shah, K.S.; Roy, U.N.; Burger, A.; Boatner, L.A.; et al. Strontium and barium iodide high light yield scintillators. *Appl. Phys. Lett.* **2008**, *92*, 083508. [CrossRef]
25. Mizoi, K.; Arai, M.; Fujimoto, Y.; Nakauchi, D.; Koshimizu, M.; Yanagida, T.; Asai, K. Evaluation of photoluminescence and scintillation properties of Yb^{2+}-doped $SrCl_{2-x}Br_x$ crystals. *J. Ceram. Soc. Jpn.* **2021**, *129*, 406–414. [CrossRef]
26. He, Z.; Wang, Y.; Li, S.; Xu, X. Dynamic studies on the time-resolved fluorescence of Sm^{2+} in $BaCl_2$. *J. Lumin.* **2002**, *97*, 102–106. [CrossRef]
27. Dixie, L.C.; Edgar, A.; Reid, M.F. Sm^{2+} fluorescence and absorption in cubic $BaCl_2$: Strong thermal crossover of fluorescence between $4f^6$ and $4f^55d^1$ configurations. *J. Lumin.* **2012**, *132*, 2775–2782. [CrossRef]
28. Karbowiak, M.; Solarz, P.; Lisiecki, R.; Ryba-Romanowski, W. Optical spectra and excited state relaxation dynamics of Sm^{2+} ions in $SrCl_2$, $SrBr_2$ and SrI_2 crystals. *J. Lumin.* **2018**, *195*, 159–165. [CrossRef]
29. Dixie, L.C.; Edgar, A.; Bartle, M.C. Spectroscopic and radioluminescence properties of two bright X-ray phosphors: Strontium barium chloride doped with Eu^{2+} or Sm^{2+} ions. *J. Lumin.* **2014**, *149*, 91–98. [CrossRef]
30. Dixie, L.C.; Edgar, A.; Bartle, C.M. Samarium doped calcium fluoride: A red scintillator and X-ray phosphor. *Nucl. Instrum. Methods Phys. Res. A* **2014**, *753*, 131–137. [CrossRef]
31. Awater, R.H.P.; Alekhin, M.S.; Biner, D.A.; Krämer, K.W.; Dorenbos, P. Converting SrI_2:Eu^{2+} into a near infrared scintillator by Sm^{2+} co-doping. *J. Lumin.* **2019**, *212*, 1–4. [CrossRef]
32. Wolszczak, W.; Krämer, K.W.; Dorenbos, P. $CsBa_2I_5$:Eu^{2+},Sm^{2+}—The First High-Energy Resolution Black Scintillator for γ-Ray Spectroscopy. *Phys. Status Solidi Rapid Res. Lett.* **2019**, *13*, 201900158. [CrossRef]

33. Alekhin, M.S.; Awater, R.H.P.; Biner, D.A.; Krämer, K.W.; De Haas, J.T.M.; Dorenbos, P. Luminescence and spectroscopic properties of Sm^{2+} and Er^{3+} doped SrI_2. *J. Lumin.* **2015**, *167*, 347–351. [CrossRef]
34. Nakauchi, D.; Fujimoto, Y.; Kato, T.; Kawaguchi, N.; Yanagida, T. X- And γ-ray response of Sm-doped $SrBr_2$ crystalline scintillators emitting red-NIR photons. *Jpn. J. Appl. Phys.* **2021**, *60*, 092002. [CrossRef]
35. Kanchana, V.; Vaitheeswaran, G.; Svane, A. Calculated structural, elastic and electronic properties of $SrCl_2$. *J. Alloys Compd.* **2008**, *455*, 480–484. [CrossRef]
36. Chaminade, J.P.; Viraphong, O.; Guillen, F.; Fouassier, C.; Czirr, B. Crystal growth and optical properties of new neutron detectors Ce^{3+}:$Li_6R(BO_3)_3$ (R=Gd,Y). *IEEE Trans. Nucl. Sci.* **2001**, *48*, 1158–1161. [CrossRef]
37. Yanagida, T.; Kamada, K.; Fujimoto, Y.; Yagi, H.; Yanagitani, T. Comparative study of ceramic and single crystal Ce:GAGG scintillator. *Opt. Mater.* **2013**, *35*, 2480–2485. [CrossRef]
38. Yanagida, T.; Fujimoto, Y.; Ito, T.; Uchiyama, K.; Mori, K. Development of X-ray-induced afterglow characterization system. *Appl. Phys. Express* **2014**, *7*, 062401. [CrossRef]
39. Antonyak, O.T.; Chornodolskyy, Y.M.; Syrotyuk, S.V.; Gloskovska, N.V.; Gamernyk, R. V High-energy electronic excitations and radiation defects in $SrCl_2$ crystals. *Mater. Res. Express* **2017**, *4*, 116306. [CrossRef]
40. Yanagida, T.; Takahashi, H.; Ito, T.; Kasama, D.; Enoto, T.; Sato, M.; Hirakuri, S.; Kokubun, M.; Makishima, K.; Yanagitani, T.; et al. Evaluation of properties of YAG (Ce) ceramic scintillators. *IEEE Trans. Nucl. Sci.* **2005**, *52*, 1836–1841. [CrossRef]
41. Bourret-Courchesne, E.D.; Bizarri, G.A.; Borade, R.; Gundiah, G.; Samulon, E.C.; Yan, Z.; Derenzo, S.E. Crystal growth and characterization of alkali-earth halide scintillators. *J. Cryst. Growth* **2012**, *352*, 78–83. [CrossRef]
42. Robbins, D.J. On Predicting the Maximum Efficiency of Phosphor Systems Excited by Ionizing Radiation. *J. Electrochem. Soc.* **1980**, *127*, 2694–2702. [CrossRef]
43. Lempicki, A.; Wojtowicz, A.J.; Berman, E. Fundamental limits of scintillator performance. *Nucl. Instrum. Methods Phys. Res. A* **1993**, *333*, 304–311. [CrossRef]